Received: 3 July 2022 | Revised: 1 August 2022 | Accepted: 3 August 2022

DOI: 10.1002/pat.5836

RESEARCH ARTICLE

polymers advanced technologies WILEY

A novel nanofibrous film with antibacterial, antioxidant, and thermoregulatory functions fabricated by coaxial electrospinning

Tianliang Dai[1] | Zhuofan Qin[1] | Shuoshuo Wang[1] | Lina Wang[1] | Juming Yao[1] | Guocheng Zhu[1] | Baochun Guo[2] | Jiri Militky[3] | Mohanapriya Venkataraman[3] | Ming Zhang[1]

[1]Zhejiang-Czech Joint Laboratory of Advanced Fiber Materials, Zhejiang Sci-Tech University, Hangzhou, China

[2]Department of Polymer Materials and Engineering, South China University of Technology, Guangzhou, China

[3]Department of Material Engineering, Faculty of Textile Engineering, Technical University of Liberec, Liberec, Czech Republic

Correspondence
Ming Zhang, Zhejiang-Czech Joint Laboratory of Advanced Fiber Materials, Zhejiang Sci-Tech University, Hangzhou, China.
Email: zhangming@zstu.edu.cn

Funding information
111 Project, Grant/Award Number: D21011; China education association for international 278 exchange, Grant/Award Number: 202020; Zhejiang Provincial Key Research and Development Program; Zhejiang Provincial Key Research Development Program, Grant/Award Number: 2022C03093

Abstract

Ordinary packaging film only has the functions of storing food and transporting food, while the external environment can affect the storage period of food. In this study, a common degradable material, polylactic acid (PLA), was chosen as the base material, and the material was endowed with antibacterial function by adding curcumin (Cur). Coaxial electrostatic spinning technology has a unique advantage in the preparation of core-sheath structured fibers, and a PLA/Cur/n-octadecane (OD) phase change thermoregulation fiber was prepared by selecting OD as the core material, which gives the fiber film thermoregulation function. The fiber structure, mechanical properties, and thermal properties were characterized. The antibacterial activity of the composite films against *Escherichia coli* and *Staphylococcus aureus* was investigated. The temperature regulation function of the composite film was evaluated, and the unique core-sheath structure endowed the fiber film with a temperature regulation function. The storage of bananas was studied in which to explore the effect on food preservation. The composite films showed excellent bactericidal as well as antioxidant properties and successfully delayed the warming phenomenon.

KEYWORDS
antibacterial and antioxidant properties, coaxial electrospinning, curcumin, food packaging, PLA, thermal regulating

1 | INTRODUCTION

As one of the cornerstones of human existence, we have come to understand the importance of food safety.[1] Traditional food packaging can no longer meet the high human standards for food preservation. Therefore, it is imperative to develop functional food packaging. A great deal of effort is currently directed to food preservation and storage management, including the incorporation of biological antimicrobial substances in packaging films[2] and the development of edible films,[3] coatings,[4] and so forth.

PLA is widely used in food packaging because of its biocompatibility, biodegradability, and excellent mechanical properties.[5–8] Ramos et al.[9] developed a PLA-based nanocomposite film with thymol and silver nanoparticles. Explored its degradation performance by burying it in compost and found that its weight loss had reached 90% after 14 days reflecting its good degradability. Therefore, numerous studies have been conducted to combine antimicrobial components from plants with PLA films to produce packaging films with excellent antimicrobial properties. As a plant extract, curcumin is a natural antimicrobial agent, and as an additional ingredient in food

packaging, there is no need to worry about its toxicity to humans.[10–12] Roy et al.[13] prepared a curcumin polylactic acid composite film by solution casting method, which has excellent flexibility and transparency, as well as antioxidant and antibacterial properties, and is a food packaging film with great potential for development. However, in addition to microbial interference, changes in temperature during the storage or transportation of food can also affect its storage cycle. Coaxial electrostatic spinning technology is a means that can be used to prepare core-sheath structured fiber films.[14–16] Phase change materials (PCMs) are loaded into various nanoscale carriers or encapsulated which are phase change fibers. Spinning PCMs as core material can obtain phase change thermoregulated fiber.[17–19] The n-octadecane undergoes a phase change at ~27°C and is an ideal material for temperature regulation under ambient conditions. Qin et al.[20] prepared a PAN/Cur@OD composite fiber film by coaxial electrostatic spinning technology, which has excellent antibacterial properties and temperature regulation, and this multifunctional composite fiber film has potential applications in the fields of clothing fabrics, preservation and storage quality of functional foods, and biomedical products.

In this work, coaxial electrostatic spinning was carried out by mixing PLA and Cur as the sheath material and OD as the core material. The kind of core-sheath structure nanofiber film with antibacterial, antioxidant, and thermoregulatory functions was successfully prepared. The antibacterial effects of the composite films were evaluated against Gram-positive and Gram-negative bacteria. The antioxidant properties of the composite films were confirmed by free radical scavenging experiments and further confirmed by storage experiments on bananas. The temperature regulation performance was evaluated by differential scanning calorimetry (DSC) and infrared thermography. The DSC test showed that the composite film has a high latent heat value, and the infrared thermography showed that the material has a good thermal temperature delay effect.

2 | EXPERIMENTAL PROCEDURE

2.1 | Materials

PLA (Mw = 160,000) was purchased from Natureworks Co., Ltd. America. NaCl and N, N-dimethyl formamide (DMF) were purchased from Hangzhou Gaojing Fine Chemical Industry Co., Ltd. N,N-dimethylacetamide (DMAc) was purchased from Macklin Biochemical Technology Co., Ltd. Acetone was purchased from Hangzhou Shuanglin Chemical Reagent Co., Ltd. Petroleum ether (AR, bp 90–120°C) and OD (99%, melting temperature is around 28°C) were purchased from Aladdin Chemistry Co., Ltd. Cur (AR, Mw = 368.38 Da) was purchased from Ron's reagent. 2,2-Diphenyl-1-picrylhydrazyl (DPPH) was purchased from Macklin Biochemical Technology Co., Ltd. Agar powder and peptone were purchased from Hangzhou Baisi Biotechnology Co., Ltd. Yeast infusion powder was purchased from Macklin Biochemical Technology Co., Ltd.

2.2 | Preparation of PLA/Cur@OD composite film

We utilize coaxial electrostatic spinning technology to prepare PLA/Cur@OD core-sheath structure composite film. To obtain the sheath solution, 14 wt% PLA and different concentrations of curcumin (1, 3, 5, and 7 wt%) were added to DMF/DMAc (1 wt% NaCl)/acetone with a ratio of 3:1:1, and magnetically stirred for 12 h in 60°C. NaCl was used to regulate fiber morphology (Figure S2). The core material is OD (Heated in the oven for 30 min before use). The spinning equipment is assembled as shown in Figure 1. The voltage and the distance from the needle tip to the collector were 20 kV and 18 cm, respectively. The sheath feed rate was 0.6 ml/h, and the core feed rate was 0.05, 0.075, 0.1, and 0.125 ml/h, respectively. The temperature adjustment system controls the ambient temperature at around 40°C, and the relative humidity is controlled at around 20% by the dehumidifier. After spinning, all the electrospinning films were heated in a vacuum oven for 30 min to remove residual solvents.

2.3 | Characterization and properties of the film

2.3.1 | Nanofibers morphology

Use the field emission-scanning electron microscope (ULTRA55, Zeiss) to observe the surface morphology of the nanofibers, and the acceleration voltage is 3 kV. All the samples are coated with a thin layer of gold. Use Image-J software to measure the diameters of 50 random fibers.

The core-sheath structure of the nanofibers is investigated by field emissiontransmission-electron microscopy (JEM-2100, JOEL) at an accelerating voltage of 120 kV. Nanofibers are deposited directly

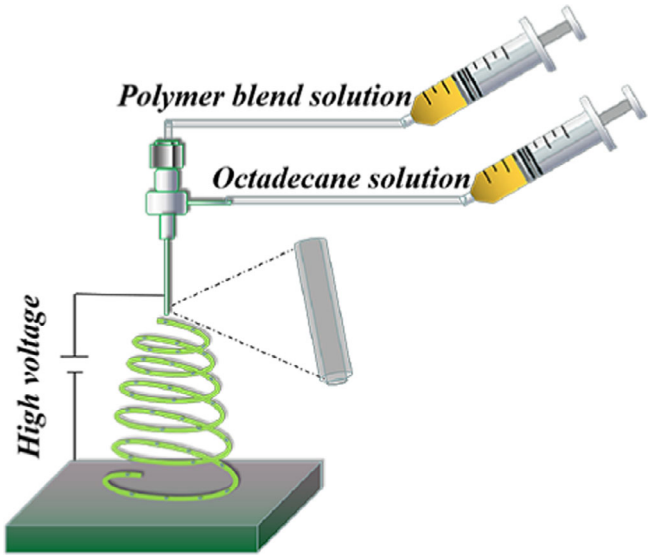

FIGURE 1 Schematic diagram of coaxial electrospinning[30]

on 400 mesh carbon-coated copper grids, and then the copper grids are presoak in petroleum ether for 24 h to remove n-octadecane.

2.3.2 | Fourier transform infrared analysis

The Fourier transform infrared spectra of the composite film samples were recorded with an FTIR spectrophotometer (Nicolet Nexus-560, Madison, WI, USA) at a wavenumber of 4000–500 cm^{-1} with the resolution of 32 scans at 4 cm^{-1}.

2.3.3 | Mechanical properties

The thickness of the film was determined using a digital micrometer (Digimatic Micrometer, Everte, Bonte Gauge Co.) with an accuracy of 1 μm. The thickness was measured at five random locations of each film and their average value was used.

Measured tensile properties by multifunctional mechanical tester (DFT) with a tensile rate of 0.1 cm/s at 25°C. The samples are cut into small pieces of 0.5 × 2 cm.

2.3.4 | Water vapor permeability and water contact angle

According to the method of Kurek et al.[21] by sealing the film samples with vulcanized rubber bands on glass bottles containing a certain amount of distilled water (8.5 cm deep without the mouth, 1 cm bottle mouth height, 1.8 cm inside diameter of the bottle mouth). Then, the test vessel was placed in an environment with 25°C and 70% relative humidity. The mass of the test vessel was recorded before and after 24 h to obtain the mass of distilled water lost, each sample was averaged for three tests, and the water vapor permeability (WVP) performance was calculated using the following equation:

$$\mathrm{WVP} = \frac{\Delta m \times \alpha}{T \times A \times \Delta P}, \tag{1}$$

where Δm (g) is the mass of water lost, α (m) is the thickness of the film, T (s) is the time used for the test, and A (m^2) is the area that water vapor can come in contact with the film, and ΔP (Pa) is the water vapor pressure difference between the two sides of the film, and ΔP was 8113 Pa at 25°C.

Testing the water contact angle of films using a video contact angle tester (JY-82A, Chengde Dingsheng Testing Equipment Co.). The film samples were cut to a size of 1 cm × 1 cm and placed on the horizontal movable table of the water contact angle (WCA) analyzer. Subsequently, a drop of water was added to the film's surface with a micro syringe, and three spots were taken for each sample, the WCA values were measured twice on both sides of each drop and the average values were reported.

2.3.5 | Thermal properties

DSC (Q2000) is carried out in nitrogen flow with a heating and cooling rate of 10 K/min. Samples are heated from 5 to 50°C and cooled from 50 to 5°C.

The maximum encapsulation rate of the PCM is calculated by the following equation:

$$\text{Encapsulation ratio}\,(\%) = \frac{\triangle H_{\mathrm{m,PCF}}}{\triangle H_{\mathrm{m,PCM}}} \times 100\%, \tag{2}$$

where $\triangle H_{\mathrm{m,PCF}}$ represents the melting enthalpy values of the PCFs with different core feed rates, and $\triangle H_{\mathrm{m,PCM}}$ represents the melting enthalpy values of the OD.

Obtained the nanofiber film's thermal stability and decomposition properties through TGA (L81/1750, LINSEIS Company).

2.3.6 | Delayed thermal response

Infrared thermography to check the actual temperature regulation of coaxial electrospinning PLA/Cur_7@$OD_{0.1}$ film. The real-time temperature change of PLA/Cur_7 film and coaxial electrospinning PLA/-Cur_7@$OD_{0.1}$ film under the baking lamp observed by infrared thermography. The temperature change was recorded every 5 s.

2.4 | The antibacterial experiment

Through the colony counting method to represent the antibacterial performance. First, the original *Staphylococcus aureus* colonies and *Escherichia coli* colonies were inoculated into a peptone liquid medium and placed in a shaker, and incubated at 37°C and 220 rpm for 24 h to obtain the initial bacterial solution. The initial concentration of the bacterial solution is approximately 10^{-8} CFU/ml. After diluting the bacterial solution to 10^{-3} CFU/ml, 40 mg of the composite film with different Cur concentrations was added to it. Pure PLA film and the film-less bacterial solution were set as a blank control (Figure S5). The antimicrobial test was performed in triplicate with individually prepared films. After shaking, the film was added into a 5 ml centrifuge tube and fully contacted with the bacterial liquid. Then it was placed in a 38°C shaker for 8 h at a speed of 100 rpm. For the *E. coil*, the samples were taken out at predetermined time intervals (0, 2, 4, 6, and 8 h) of incubation, and 100 μl of bacterial solution were taken and coated on an agar medium. For the *S. aureus*, they were taken out at time intervals (0, 1, 2, 3, 4, and 5 h) of incubation. After coating, the solid medium was incubated in a thermostat at 38°C for 24 h. After 24 h, take them out and count them with colony counting software. All experiments were conducted in a sterile environment. The Bacteria inhibition rate was calculated as follows:

$$\text{Bacteria inhibition rate} = \frac{B_c - B_s}{B_c} \times 100\%, \tag{3}$$

where B_c and B_s represent the number of colonies before and after contact between the antibacterial film and the bacterial solution.

2.5 | The antioxidant experiment

Antioxidant activity of PLA/Cur composite films was measured by 2,2-diphenyl-1-picrylhydrazyl radical (DPPH•) radical scavenging assay. First, prepare 100 ml of 0.1 mM DPPH• ethanol solution. For DPPH• analysis of composite films, 35 mg of film samples with different Cur concentrations (0, 1, 3, 5, and 7 wt%) were placed in 4 ml of DPPH• solution and incubated for 3 h at room temperature. The same film-less DPPH• solution was used for the control group. After incubation, the absorbance was measured at 517 nm using a UV spectrophotometer, and the antioxidant activity of the film was calculated using the following equation:

$$\text{Free radical scavenging activity}\,(\%) = \frac{A_c - A_s}{A_c} \times 100, \qquad (4)$$

where A_C represents the UV absorbance of DPPH solution, and A_S represents the UV absorbance of DPPH• solution after adding PLA/Cur composite film.

2.6 | The visual antioxidation experiment

Wrap fresh bananas of uniform batch production with 52 × 22 (cm) size film and take them out after 1 week to check the internal changes of bananas. Ordinary PE bag and pure PLA film were used as blank controls, and PLA/Cur_7 was used as the experimental group (Figure S6).

2.7 | In vitro release experiment

In vitro released experiment was conducted according to the method reported by Llorens et al.[22] with slightly modification. The controlled release of curcumin from nanofibers was investigated in PBS (0.01 M, pH 7.4)/ethanol (7:3 v/v) mixture as a medium. A calibration curve was established by dissolving different concentrations of curcumin in a PBS/ethanol mixture and measuring the absorbance at 435 nm by UV spectrophotometer to determine the drug concentration for subsequent experiments. The curcumin-loaded fibers (5 mg) were placed into 30 ml of PBS/ethanol mixture at 37°C under shaking at 120 rpm. Samples were withdrawn from the release medium at predetermined time intervals. The release of curcumin was analyzed by determining the absorbance at 435 nm with a UV-spectrophotometer. The volume was kept constant by adding fresh medium. All release tests were carried out in triplicate.

2.8 | Statistical analysis

Data are presented as mean ± standard error of the mean and represented for three independent experiments. The statistical significance of mean values between multiple treatment groups was accessed by one-way analysis of variance (ANOVA) with Tukey's test. p value <0.05 was considered statistically significant.

3 | RESULTS AND DISCUSSION

3.1 | Morphologies of the electrospinning nanofibers

Figure S2 shows the SEM images of PLA composite films, and it can be seen that the fiber morphology is smooth without the presence of beads, and the fiber diameter increases with the growth of curcumin content and the wrapping of octadecane.

Through antibacterial experiments, it was found that the best antibacterial effect was achieved when the curcumin content was 7 wt%, so we chose 7 wt% curcumin concentration for coaxial electrostatic spinning. Figure 2 shows the TEM images of PLA/Cur_7@$OD_{0.1}$ nanofibers, which shows that the fibers form a bamboo-like core-sheath structure, confirming the successful encapsulation of n-octadecane into the fibers.

3.2 | FT-IR analysis

The FTIR spectra of curcumin, n-octadecane, PLA/Cur composite films and coaxial electrospun PLA/Cur@OD films are shown in Figure S3. In the spectrum of PLA, a broad and weak peak appears at 3440 cm^{-1}, which may be due to the chalet -OH. the weak peak near 2997 cm^{-1} is due to the stretching vibration of C-H. The peaks found at 1184 and 1087 cm^{-1} were due to the symmetric and asymmetric stretching of the complex C—O—C group, respectively.[13] The peak at 1752 cm^{-1} was attributed to the stretching vibration of C═O in the —COOH group.[23] For the spectra of curcumin, the peaks observed at 1627 and 1510 cm^{-1} were attributed to the carbonyl and ethylene groups, respectively.[24] The spectrum of the PLA/Cur composite film shows two characteristic peaks of Cur, indicating that the two substances are well combined and no excess peak pattern is produced. In the case of n-octadecane, two absorption peaks at 2920 and 2850 cm^{-1}, represent the stretching vibration of the C-H bond in -CH_2 and -CH_3. The absorption peak at 1471 cm^{-1} is the shear bending vibration of the -CH_2 group. The absorption peak at 717 cm^{-1} is the wobble vibration of the -CH_2 group, indicating that n-octadecane has a long-chain alkane structure. The spectra of the PLA/Cur@OD include all the characteristic absorption peaks of the n-octadecane, curcumin and the PLA, which indicate that there is no chemical interaction between the n-octadecane, curcumin and the PLA.

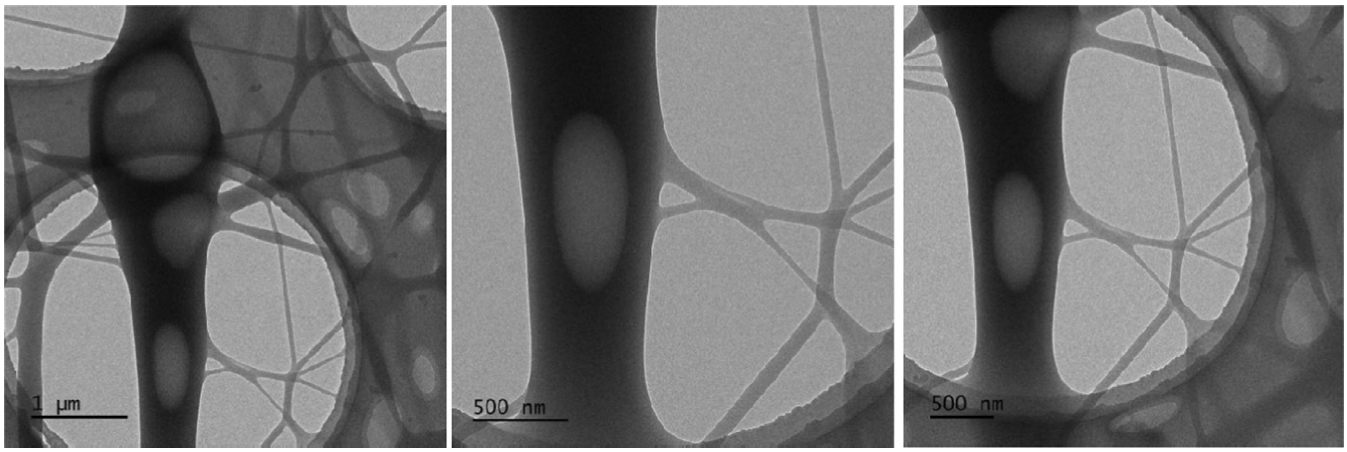

FIGURE 2 The TEM image of core-sheath structure PLA/Cur_7@$OD_{0.1}$ nanofibers

3.3 | Mechanical properties

The mechanical properties of composite films at room temperature were tested. As can be seen from Figure S4a, with the addition of curcumin, there is a decreasing trend in tensile strength, which does not show a regular change with the trend of concentration change. We speculate that it may be due to the addition of sodium chloride in the spinning solution, which led to the decrease in the mechanical properties of the material. Both Kanmani[25] and Li[26] found a decrease in the mechanical properties of the material with the addition of nanoparticles in their studies, which may be due to the weak interfacial interaction between the polymer matrix and the nanoparticles. We found that there is a little granular material on the fiber surface by SEM (Figure S7), which may confirm our conjecture. The tensile strength of n-octadecane-encapsulated composite fiber films is even lower, probably because n-octadecane crystallizes at room temperature and the molecular chains tend to be tightly arranged, leaving little space for movement. On the other hand, the elongation at the break of the composite films with the 1% concentration of curcumin was increased (Figure S4b). Ezati et al.[27] found that curcumin could be used as a plasticizer to enhance the flexibility of the polymer. As the concentration of curcumin increased, the elongation at the break of the films showed a decreasing trend, which we speculate may be due to the rigid groups contained in curcumin, where the benzene ring in curcumin forms a large number of hydrogen bonds with PLA and thus forms a cross-linked network that limits the stretching of the material. Interestingly, when we tried to encapsulate n-octadecane in the composite film, the elongation at the break of the material was improved, probably due to the long chain molecules of n-octadecane, which increased the overall flexibility of the polymer molecular chain, resulting in an increase in elongation at break.

3.4 | WVP and WCA

The WVP values of pure PLA films and PLA composite films with different curcumin contents added are shown in Table 1. The WVP of the pure PLA film was $1.876 \pm 0.150 \times 10^{-10}$ g m/m^2 Pa s. With the increase of curcumin content, the WVP of the composite films showed an increasing trend. Marra et al.[28] suggested that the use of curcumin as an additive led to a change in the free volume between PLA fibers, which in turn affected the permeability of water vapor.

WCA test results are shown in Table 1. Both pure PLA film and PLA/Cur composite films exhibited superhydrophobicity (hydrophobic angles were both over 130°). In addition, the coaxially spun PLA/-Cur@OD films also maintain superhydrophobicity, which indicates that OD does not affect the surface structure of the composite film.

3.5 | Thermal analysis

Figure S8a,b shows the DSC curves of the composite films at different core feed rates. Table 2 shows the DSC values of PCFs with different core material supply rates and n-octadecane. It can be seen that the melting-crystallization peak area increases as the core feed rate increases (Figure S8a,b), and when the core feed rate reaches 0.1 ml/h, the peak area no longer changes significantly, and the latent heat values are relatively similar (Table 2). Due to the encapsulation rate of the fiber-wrapped n-octadecane reaching a maximum (~36%). When the core flow rate is 0.05 and 0.075 ml/h, there is a slight change in the phase change behavior of the cooling process, and two peaks appear in the DSC curve. Due to the presence of multiple nucleation sites in n-octadecane during the cooling process and the formation of different crystalline phases.[29] Qin et al.[30] experimentally concluded that the appearance of bimodal peaks is related to the degree of supercooling, which in turn is related to the curvature of the n-octadecane crystalline substrate and the microstructure formed during the spinning process. With the increase in core flow rate, the encapsulation rate of n-octadecane was elevated, and the bimodal peaks disappeared. Su et al. suggested that this was because the increase of n-octadecane filled the fiber sufficiently, and the hollow structure inside the fiber could prevent the leakage of OD during the phase transition, which in turn reduced the generation of heterophase nucleation sites.[31] Figure S8c,d shows the DSC cycling test of the PLA/Cur_7@$OD_{0.1}$ film, and it can be seen that the latent heat value

TABLE 1 Thickness, water contact angle and water permeability of the composite film

Films	Thickness (μm)	WVP ($\times 10^{-10}$ g m/m^2 Pa s)	WCA (°)
PLA	101.4 ± 0.38	1.876 ± 0.05^{a}	134.3 ± 0.82^{b}
PLA/Cur$_1$	97.0 ± 0.05	2.089 ± 0.04^{ac}	134.3 ± 1.73^{b}
PLA/Cur$_3$	104.7 ± 0.65	1.969 ± 0.06^{a}	134.4 ± 0.58^{b}
PLA/Cur$_5$	104.9 ± 0.10	2.420 ± 0.16^{bc}	132.39 ± 1.95^{b}
PLA/Cur$_7$	104.0 ± 0.90	2.440 ± 0.08^{bc}	133.69 ± 0.65^{b}
PLA/Cur$_7$@OD$_{0.1}$	131.7 ± 0.75	2.644 ± 0.11^{b}	133.71 ± 0.97^{b}

Notes: a, b, c, d means with different letters within a column indicate significance difference ($p \leq 0.05$).

TABLE 2 DSC values of PLA/Cur@OD fibers with different core feed rate and n-octadecane

Samples	Core feed rate (ml/h)	Peak temperature (T_m, °C)	$\triangle H_m$ (J/g)	Peak temperature (T_c, °C)	$\triangle H_c$ (J/g)	Encapsulation rate (%)
PLA/ Cur@OD	0.05	20.78	46.28	28.67	46.04	18.15
	0.075	20.47	73.72	29.83	72.63	28.90
	0.1	19.30	93.18	30.59	89.32	36.53
	0.125	19.60	92.12	30.22	92.24	36.12
n-octadecane	–	28.36	255.03	19.76	251.3	–

Notes: a, b, c, d means with different letters within a column indicate significance difference ($p \leq 0.05$).

remains almost unchanged after nine cycles of testing, indicating that the film has good thermal cyclability.

Thermal stability of PLA, PLA/Cur$_7$, PLA/Cur$_7$@OD$_{0.1}$, curcumin, and n-octadecane, were evaluated using thermogravimetric analysis (TGA). Figure S9 shows the relationship between sample temperature and percent weight loss. The weight change was observed at 200–450°C for curcumin and 100–250°C for the n-octadecane. The neat PLA film initially decomposes at 270°C and completely decomposes at 360°C. The weight shift of PLA/Cur film occurred at 260–360°C. For the PLA/Cur$_7$@OD$_{0.1}$ composite film, its thermal degradation pattern includes two steps. At first, an apparent weight loss was observed at 120°C due to the n-octadecane decomposition. The second weight shift occurred at 270–360°C for PLA.

3.6 | Delayed thermal response

Figure 3 shows the real-time infrared thermography of PLA/Cur$_7$ composite film (A) and PLA/Cur$_7$@OD$_{0.1}$ composite film (B) on a heating table. The film A is heated from 38.5°C and B from 38.3°C. When heated for 5 s, film A rises by 2.9°C and B by 2.1°C. After heating for 10S, film A increased by 5.2°C and B by 4.3°C. Therefore, the coaxial electrostatic spun PLA/Cur$_7$@OD$_{0.1}$ composite film exhibited a delayed thermal response. After heating for 15S, film A increased to 45.8°C and B to 45.1°C. The temperature difference between them decreased, indicating that the n-octadecane in the fiber had melted.

3.7 | Antibacterial activity analysis

Gram-negative *E. coil* and Gram-positive *S. aureus* were obtained from Shanghai Luwei Technology Co. Ltd. As shown in Figure 4A,C, the antibacterial effects of pure PLA fiber membranes were compared with those of composite fiber membranes added with different Cur concentrations against *S. aureus* and *E. coli*. As the concentration of curcumin increased, the antibacterial effect of the fiber membranes also increased. When the curcumin concentration was 7 wt%, the antibacterial effect was the best, and there were almost no colonies on the culture dish, and the inhibition rate of the fiber membrane against *S. aureus* and *E. coli* was 99% and 100%, respectively. In order to verify the reliability of the experiment, the antibacterial efficiency of antibacterial films containing different concentrations of curcumin after 8 h of contact with *E. coli* bacterial solution and after 5 h of contact with *S. aureus* were repeatedly tested, and the results were consistent with the preliminary test (Figure 4B,D). In addition, the coaxial electrospinning PLA/Cur$_7$@OD$_{0.1}$ film has shown excellent antibacterial effects as well (Figure S10). Kaur et al.[32] investigated the bactericidal mechanism of curcumin. The cytoskeletal protein FtsZ is present in most bacteria and plays a key role in prokaryotic cell division. They found that curcumin could inhibit the polymerization of FtsZ and thus showed antibacterial activity. Through the study of Liu[33] and Kumar[34] et al., we know that curcumin released from the composite membrane can act directly on the cell membrane of microorganisms and destroy the cell structure, thus achieving a bactericidal effect.

The results seem to show that curcumin has a better antibacterial effect against *S. aureus* than *E. coli*. This is consistent with the previous work by other researchers.[35,36] According to previous reports, it is due to the changes caused by the difference in cell structure between Gram-positive and Gram-negative bacteria. It is believed that the stronger effect of curcumin and other natural substances on Gram-positive bacteria is due to the different structure and composition of the microbial cell walls. The cells of Gram-positive bacteria are surrounded by a thick layer of peptidoglycan containing an additional

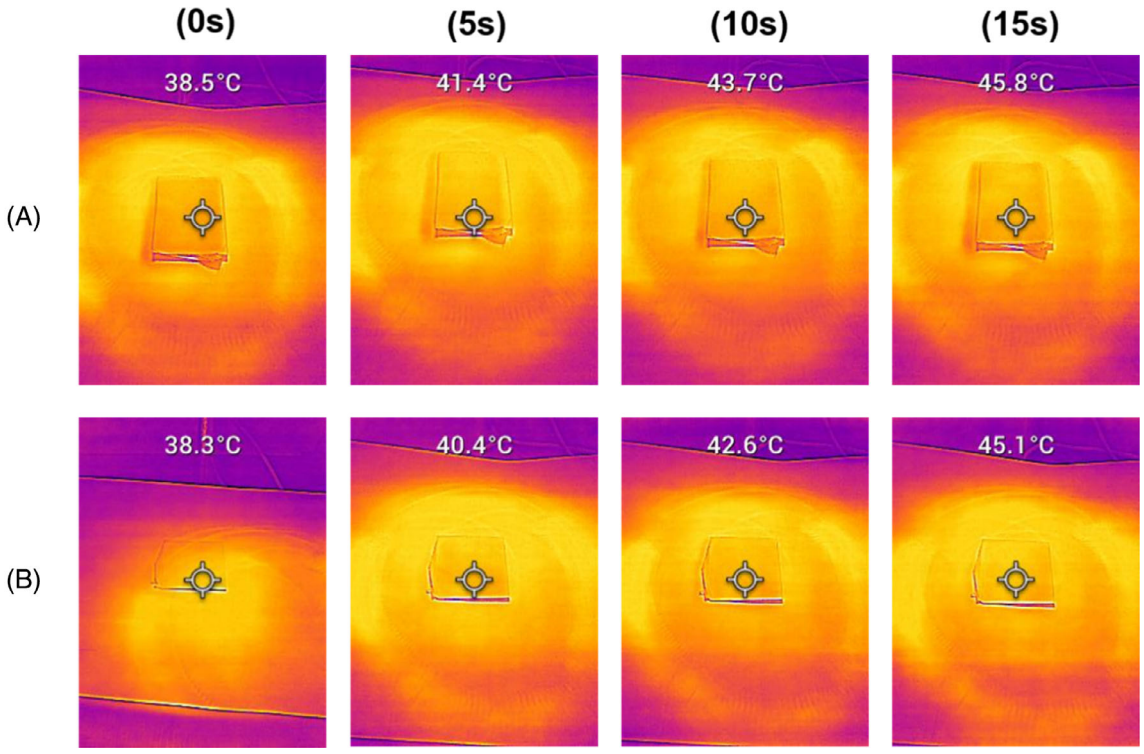

FIGURE 3 Thermographic images of samples (A) PLA/Cur_7 composite film, (B) PLA/Cur_7@$OD_{0.1}$ composite film

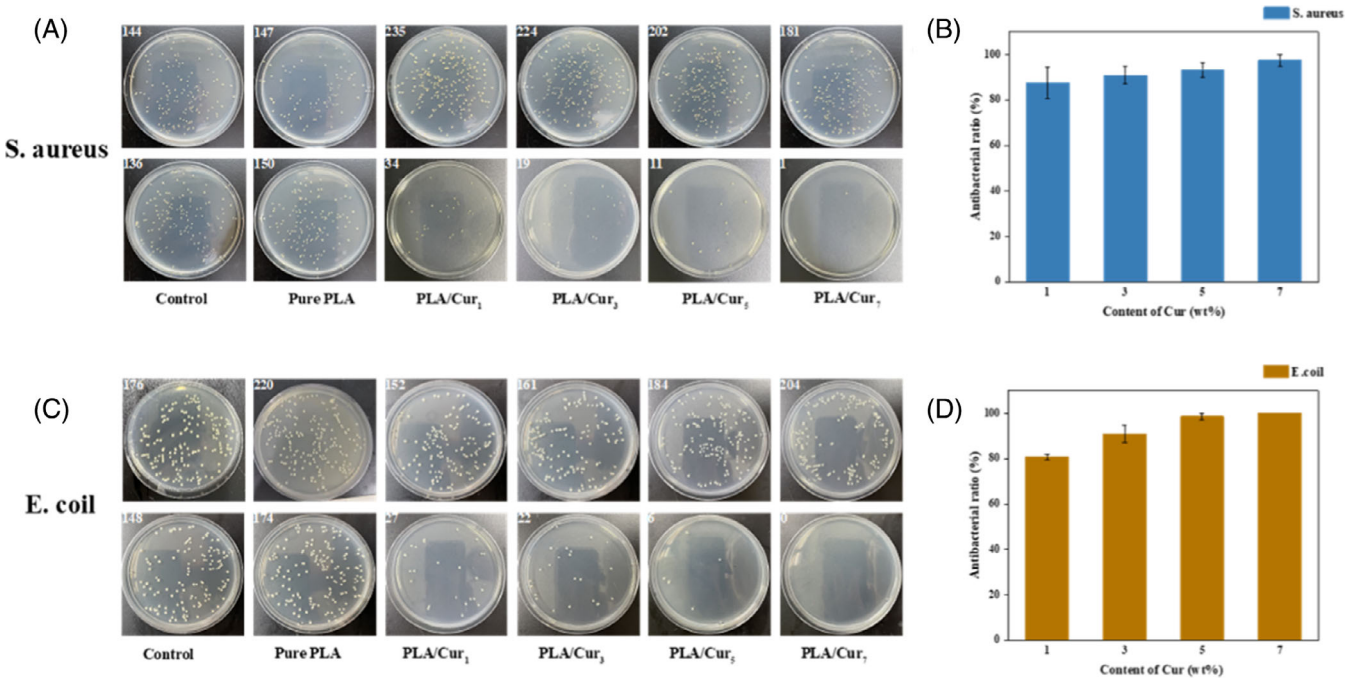

FIGURE 4 (A,C) The optical image of antibacterial effect of the fiber membranes against *Staphylococcus aureus* (5 h of contact) and *Escherichia coli* (8 h of contact), (B,D) The repeated tests of bacterial inhibition rates of antibacterial fiber films against *E. coli* and *S. aureus*

class of lipoteichoic acid, but they have no outer film. In contrast, the cell wall of Gram-negative bacteria is less thick but more complex, consisting of peptidoglycan and containing a variety of proteins, lipids, and polysaccharides. The complexity of the outer film of Gram-negative bacteria largely determines their level of resistance to antibiotics.[37–39]

3.8 | Antioxidant activity

The antioxidant activity of PLA/Cur composite film was measured by measuring the DPPH• radical scavenging activity. Results are shown in Figure S11a PLA/Cur films exhibited strong antioxidant activity, which was related to the concentration of curcumin. The DPPH• scavenging efficiency of PLA films with different curcumin contents (1, 3, 5, and 7 wt%) reached 65.12% ± 1.14%, 66.24% ± 1.55%, and 71.29% ± 1.49%, 79.40 ± 1.41%, respectively. The DPPH• radical scavenging efficiency of coaxial electrospinning PLA/Cur_7@$OD_{0.1}$ film was 71.64% ± 0.72%. Compared with PLA/Cur_7, its DPPH• scavenging efficiency was slightly decreased, which was possibly due to the decrease in curcumin content caused by the partial encapsulation of n-octadecane by the fiber. The pure PLA film has almost no free radical scavenging effect, and its UV absorption at 517 nm is comparable to that of DPPH• solution (Table 3). In addition, the effect of PLA/-Cur_7 films on the scavenging efficiency of DPPH• radicals versus time was also investigated. It was found that the UV absorbance of DPPH• at 517 nm gradually decreased with increasing time (Figure S11b), which may be due to the increase in time, more curcumin was released from the film and enhanced the scavenging efficiency of DPPH•.

3.9 | The visual antioxidation experiment

Figure 5 shows the oxidative decay inside the bananas after wrapping them in different packages for 1 week. It can be seen that the bananas wrapped with the PLA/Cur_7 packaging film remained fresh inside, while the curcumin-free PLA packaging film showed some decay, and the bananas wrapped with ordinary plastic bag had severe decay. This indicates that PLA/Cur packaging film can extend the shelf life of bananas.

3.10 | In vitro release experiment

The results of in vitro releasing curcumin to PBS/ethanol mixture from the PLA/Cur (1, 3, 5, and 6 wt%) and PLA/Cur_7@$OD_{0.1}$ composite films are shown in Figure S12. All the composite films had curcumin released at the moment of contact with the mixed media, which was due to a large amount of curcumin attached to the fiber surface. The release rate of curcumin gradually decreased with the increase of time, and the release rate decreased in a stepwise manner due to the reduction of curcumin content in the composite film.

TABLE 3 UV absorbance of the composite film added to the DPPH• solution

Samples	DPPH• solution	PLA film	PLA/Cur_1	PLA/Cur_3	PLA/Cur_5	PLA/Cur_7	PLA/Cur_7@$OD_{0.1}$
Absorbance	1.034 ± 0.009^a	1.020 ± 0.005^a	0.360 ± 0.008^b	0.349 ± 0.010^b	0.297 ± 0.012^c	0.213 ± 0.012^d	0.293 ± 0.004^c

Notes: a, b, c, d means with different letters within a column indicate significance difference ($p \leq 0.05$).

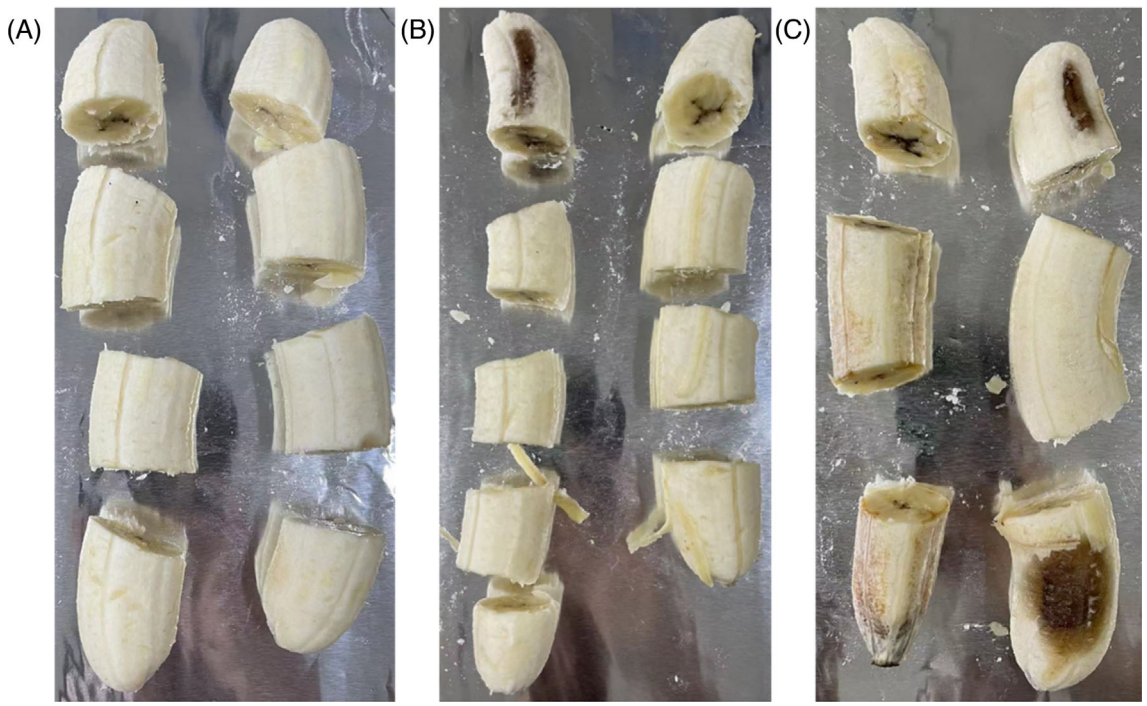

FIGURE 5 Internal changes of bananas wrapped in different packaging films after 1 week (A) PLA/Cur_7 film, (B) PLA film, (C) ordinary plastic bag

4 | CONCLUSIONS

In conclusion, we prepared nanofiber films with antibacterial, antioxidant, and thermoregulatory functions by coaxial electrostatic spinning. Curcumin in PLA fibers resulted in excellent antibacterial function and antioxidant effect, which successfully delayed the decay of bananas. TEM images showed that PLA/Cur@OD fibers had a core-sheath structure, and the polymer successfully wrapped n-octadecane, which imparted the thermal regulation function of the fibers. Infrared thermography also illustrated that the core-sheath structured composite film had a delayed thermal response. The antibacterial effect remained excellent after the polymer loading of n-octadecane, indicating that the composite film has the potential to become a new generation of smart antibacterial and antioxidant thermoregulated packaging. Therefore, this study also provides a new idea for the development of future food packaging.

ACKNOWLEDGMENT

This study was supported by the 111 Project (D21011), China Education Association for International 278 Exchange (Grant No. 202020), and Zhejiang Provincial Key Research Development Program (2022C03093).

CONFLICT OF INTEREST

The authors declare no conflict of interest.

DATA AVAILABILITY STATEMENT

The datasets generated or analyzed during this study are available from the corresponding author on reasonable request.

ORCID

Mohanapriya Venkataraman https://orcid.org/0000-0002-8977-1244

Ming Zhang https://orcid.org/0000-0002-2916-8128

REFERENCES

1. Walls H, Baker P, Chirwa E, Hawkins B. Food security, food safety & healthy nutrition: are they compatible? *Glob Food Sec*. 2019;21:69-71.
2. Mahato N, Sharma K, Koteswararao R, Sinha M, Baral E, Cho MH. Citrus essential oils: extraction, authentication and application in food preservation. *Crit Rev Food Sci Nutr*. 2019;59(4):611-625.
3. Yong H, Liu J. Active packaging films and edible coatings based on polyphenol-rich propolis extract: a review. *Compr Rev Food Sci Food Saf*. 2021;20(2):2106-2145.
4. Zhang X, Ismail BB, Cheng H, et al. Emerging chitosan-essential oil films and coatings for food preservation—a review of advances and applications. *Carbohydr Polym*. 2021;273:118616.
5. Chen Y, Geever LM, Killion JA, Lyons JG, Higginbotham CL, Devine DM. Review of multifarious applications of poly(lactic acid). *Polym-Plast Technol Eng*. 2016;55(10):1057-1075.
6. Gan I, Chow WS. Antimicrobial poly(lactic acid)/cellulose bionanocomposite for food packaging application: a review. *Food Packag Shelf Life*. 2018;17:150-161.
7. Muller J, González-Martínez C, Chiralt A. Combination of poly(lactic) acid and starch for biodegradable food packaging. *Materials*. 2017;10(8):952.
8. Goh K, Heising JK, Yuan Y, et al. Sandwich-architectured poly(lactic acid)–graphene composite food packaging films. *ACS Appl Mater Interfaces*. 2016;8(15):9994-10004.
9. Ramos M, Fortunati E, Peltzer M, Jimenez A, Kenny JM, Garrigós MC. Characterization and disintegrability under composting conditions of PLA-based nanocomposite films with thymol and silver nanoparticles. *Polym Degrad Stab*. 2016;132:2-10.
10. Hussain Y, Alam W, Ullah H, et al. Antimicrobial potential of curcumin: therapeutic potential and challenges to clinical applications. *Antibiotics*. 2022;11(3):322.
11. Silva AC, Santos PDF, Silva JTP, Leimann FV, Bracht L, Gonçalves OH. Impact of curcumin nanoformulation on its antimicrobial activity. *Trends Food Sci Technol*. 2018;72:74-82.
12. Dai C, Lin J, Li H, et al. The natural product curcumin as an antibacterial agent: current achievements and problems. *Antioxidants*. 2022;11(3):459.
13. Roy S, Rhim JW. Preparation of bioactive functional poly(lactic acid)/-curcumin composite film for food packaging application. *Int J Biol Macromol*. 2020;162:1780-1789.
14. Tong H-W, Zhang X, Wang M. A new nanofiber fabrication technique based on coaxial electrospinning. *Mater Lett*. 2012;66(1):257-260.
15. Li J, Liu Y, Abdelhakim HE. Drug delivery applications of coaxial electrospun Nanofibres in cancer therapy. *Molecules*. 2022;27(6):1803.
16. Qu H, Wei S, Guo Z. Coaxial electrospun nanostructures and their applications. *J Mater Chem A*. 2013;1(38):11513-11528.
17. Wang S, Chen W, Wang L, et al. Multifunctional nanofiber membrane with anti-ultraviolet and thermal regulation fabricated by coaxial electrospinning. *J Ind Eng Chem*. 2022;108:449-455.
18. Youssef R, Hosen MS, He J, Al-Saadi M, Van Mierlo J, Berecibar M. Thermal performance improvement for different strategies of battery thermal management systems combined with jute—a comparison study. *Energies*. 2022;15(3):873.
19. Youssef R, Hosen MS, He J, Al-Saadi M, Van Mierlo J, Berecibar M. Novel design optimization for passive cooling PCM assisted battery thermal management system in electric vehicles. *Case Stud Therm Eng*. 2022;32:101896.
20. Qin Z, Wang S, Wang L, et al. Nanofibrous membranes with antibacterial and thermoregulatory functions fabricated by coaxial electrospinning. *J Ind Eng Chem*. 2022;113:373-379.
21. Kurek M, Garofulić IE, Bakić MT, Ščetar M, Uzelac VD, Galić K. Development and evaluation of a novel antioxidant and pH indicator film based on chitosan and food waste sources of antioxidants. *Food Hydrocoll*. 2018;84:238-246.
22. Llorens E, Ibañez H, del Valle LJ, Puiggalí J. Biocompatibility and drug release behavior of scaffolds prepared by coaxial electrospinning of poly(butylene succinate) and polyethylene glycol. *Mater Sci Eng C*. 2015;49:472-484.
23. Wang H, Liu H, Chu C, et al. Diffusion and antibacterial properties of Nisin-loaded chitosan/poly(L-lactic acid) towards development of active food packaging film. *Food Bioprocess Technol*. 2015;8(8):1657-1667.
24. Roy S, Rhim J-W. Carboxymethyl cellulose-based antioxidant and antimicrobial active packaging film incorporated with curcumin and zinc oxide. *Int J Biol Macromol*. 2020;148:666-676.
25. Kanmani P, Rhim J-W. Properties and characterization of bionanocomposite films prepared with various biopolymers and ZnO nanoparticles. *Carbohydr Polym*. 2014;106:190-199.
26. Li JH, Hong RY, Li MY, Li HZ, Zheng Y, Ding J. Effects of ZnO nanoparticles on the mechanical and antibacterial properties of polyurethane coatings. *Prog Org Coat*. 2009;64(4):504-509.
27. Ezati P, Rhim JW. pH-responsive pectin-based multifunctional films incorporated with curcumin and sulfur nanoparticles. *Carbohydr Polym*. 2020;230:115638.

28. Marra A, Silvestre C, Duraccio D, Cimmino S. Polylactic acid/zinc oxide biocomposite films for food packaging application. *Int J Biol Macromol*. 2016;88:254-262.
29. Methaapanon R, Kornbongkotmas S, Ataboonwongse C, Soottitantawat A. Microencapsulation of n-octadecane and methyl palmitate phase change materials in silica by spray drying process. *Powder Technol*. 2020;361:910-916.
30. Qin Z, Yi L, Wang S, et al. Supercooling suppression and mechanical property improvement of phase change nanofibers by optimizing core distribution. *Polymer*. 2021;233:124176.
31. Su Y, Liu G, Xie B, Fu D, Wang D. Crystallization features of normal alkanes in confined geometry. *Acc Chem Res*. 2014;47(1):192-201.
32. Kaur S, Modi NH, Panda D, Roy N. Probing the binding site of curcumin in *Escherichia coli* and *Bacillus subtilis* FtsZ—a structural insight to unveil antibacterial activity of curcumin. *Eur J Med Chem*. 2010;45(9):4209-4214.
33. Liu D, Dang S, Zhang L, Munsop K, Li X. Corn starch/polyvinyl alcohol based films incorporated with curcumin-loaded Pickering emulsion for application in intelligent packaging. *Int J Biol Macromol*. 2021;188:974-982.
34. Kumar P, Kandi SK, Manohar S, Mukhopadhyay K, Rawat DS. Monocarbonyl Curcuminoids with improved stability as antibacterial agents against *Staphylococcus aureus* and their mechanistic studies. *ACS Omega*. 2019;4(1):675-687.
35. Adamczak A, Ozarowski M, Karpinski TM. Curcumin, a natural antimicrobial agent with strain-specific activity. *Pharmaceuticals*. 2020;13(7):153.
36. Subbuvel M, Kavan P. Development and investigation of antibacterial and antioxidant characteristics of poly lactic acid films blended with neem oil and curcumin. *J Appl Polym Sci*. 2021;139(14):e51891.
37. Breijyeh Z, Jubeh B, Karaman R. Resistance of gram-negative bacteria to current antibacterial agents and approaches to resolve it. *Molecules*. 2020;25(6):1340.
38. Burt S. Essential oils: their antibacterial properties and potential applications in foods—a review. *Int J Food Microbiol*. 2004;94(3):223-253.
39. Vahedikia N, Garavand F, Tajeddin B, et al. Biodegradable zein film composites reinforced with chitosan nanoparticles and cinnamon essential oil: physical, mechanical, structural and antimicrobial attributes. *Colloids Surf B: Biointerfaces*. 2019;177:25-32.

SUPPORTING INFORMATION

Additional supporting information can be found online in the Supporting Information section at the end of this article.

How to cite this article: Dai T, Qin Z, Wang S, et al. A novel nanofibrous film with antibacterial, antioxidant, and thermoregulatory functions fabricated by coaxial electrospinning. *Polym Adv Technol*. 2022;33(12):4062-4071. doi:10.1002/pat.5836